

Preliminary Simulations of the Ullage Dynamics in Microgravity during the Jet Mixing Portion of Tank Pressure Control Experiments

Kevin Breisacher¹ and Jeffrey Moder²

NASA Glenn Research Center, Cleveland, Ohio 44135

The results of CFD simulations of microgravity tank pressure control experiments performed on the Space Shuttle are presented. A 13.7 L acrylic model tank was used in these experiments. The tank was filled to an 83% fill fraction with Freon refrigerant to simulate cryogenic propellants stored in space. In the experiments, a single liquid jet near the bottom of the tank was used for mixing the tank. Simulations at a range of jet Weber numbers were performed. Qualitative comparisons of the liquid and gas interface dynamics observed and recorded in the experiments and those computed are shown and discussed. The simulations were able to correctly capture jet penetration of the ullage, qualitatively reproduce ullage shapes and dynamics, as well as the final equilibrium position of the ullage.

Nomenclature

D = diameter

R = radius

V = velocity

x = distance

We = Weber number

ρ = density

σ = surface tension

x = distance

subscripts

j = jet

l = liquid

o = nozzle outlet

I. Introduction

The Tank Pressure Control Experiment (TPCE) was a Get-Away-Special experiment flown in space on the Space Shuttle in 1991 (STS-43). Among the objectives¹ of the TPCE were to characterize the fluid dynamics of jet induced mixing in a microgravity environment and to provide data to validate computational fluid dynamic models of the mixing process. Prior to the experiment flying, Wendl et al.² made predictions of the geyser expected to be formed by the jet mixer using a 2D CFD code.

A 0.254 m diameter tank with a volume of 13.7 L was used for the experiments. The tank consisted of two hemispherical domes separated by a .102 m long cylindrical section. The tank was fabricated largely from a transparent acrylic for optical access (Figure

1.). A 0.01016 m diameter nozzle placed .063 m from the end of the tank was used to create the jet for mixing. The tank also had two internal heating elements one at the top of the dome opposite the nozzle and one at the center of the tank near the wall. The heater dimensions and placement are shown in Figure 2. At the end of the tank near the jet, a Liquid Acquisition Device (LAD) was used to obtain fluid from the tank to feed the jet. The LAD was cylindrically shaped with a height of 0.108 m, a depth of 0.0122 m, and a width of 0.0229 m. There was a 0.056 m gap between the LAD and the tank wall. The side of the LAD facing the tank wall was microetched with 0.00038 m diameter perforations and had a 21% open area fraction. The tank was filled to an 83% fill fraction with Freon r-113. The Freon equilibrium pressure (at the end of jet mixing) was approximately 4,200 Pa above the vapor pressure to simulate the characteristics of subcritical cryogenic propellants stored in space near their boiling points. Video cameras were used to record to dynamics of the liquid vapor interface. Temperatures and pressures were also recorded to enable an assessment of mixing and pressure control effectiveness. Due to storage limitations at that time (flight STS-43), only the first 2 minutes of heating (self-pressurization) were recorded with video (out of a typical 10 minutes of heating), and only the first 4 minutes of jet mixing (out of a typical 15 minutes of jet mixing) were recorded with video.

II. Test Results

The results of 38 tests were reported with jet flow rates ranging from 0.38 to 3.35 L/min. The jet Weber number used to characterize the TPCE tests was adopted from previous testing by Aydelott³:

$$We_j = \rho_l V_o^2 R_o^2 / (s D_j)$$

where

D_j - is the diameter of the jet at the interface

R_o - is the radius of the liquid jet at the nozzle outlet

V_o - is the velocity of the liquid jet at nozzle outlet

ρ_l - is the density of the liquid jet

s - is the surface tension at the interface

x - is the distance from jet nozzle outlet to liquid/vapor interface

and

$$D_j = 2R_o + 0.24x \quad (\text{for } x < 12.4 R_o)$$

$$= 0.22R_o + 0.38x \quad (\text{for } x > 12.4 R_o)$$

The jet Weber number for TPCE test runs ranged from 0.29 to 22.64 (if $x = 0.127$ m is used for all test runs). The resulting liquid/vapor interface dynamics were observed to fall into three regimes. For the TPCE tank and nozzle geometry (tank diameter to tank height ratio = 1.4, tank diameter to jet diameter ratio = 25 and $x/D_j \sim 12.5$) the following jet penetration behavior was observed from the experimental video data. Below a We_j of 1.44, the jet does not penetrate the ullage and deforms the ullage in a symmetric but unsteady fashion. For $3.1 < We_j < 4.8$, the jet is deflected to one side of the ullage and the return flow attaches to the side of the tank. In the range $4.8 < We_j < 6.3$, the flow alternates between symmetric and asymmetric flow patterns and the ullage often takes a saddle-shaped form. At $We_j > 14.5$, they observed that the saddle shape of the ullage becomes more pronounced with the flow becoming more symmetric and the ullage often forming twin peaks.

III. Simulation Setup

Transient simulations of four TPCE test runs encompassing a range of jet Weber numbers were conducted with multi-physics computational fluid dynamics (CFD) code FLOW-3D. A portion of the first 4 minutes of jet mixing (the portion recorded to video) for the selected TPCE Test Runs were simulated.

The code utilizes the Volume of Fluid (VOF) fraction and various surface tracking model options to compute the liquid vapor interface motion. The geometry was modeled on a Cartesian grid with area and volume fractions used to model solid objects. A typical

grid (Figure 3.) consisted of 95 cells each in the x and y directions and 135 cells in the z direction along the main axis of the tank for approximately 742,000 active fluid cells. Initially, the flow was assumed to be uniform with no velocity and a pressure of 41.64 kPa and a temperature of 296 K. The jet flow was implemented with a fixed velocity boundary condition and a no slip condition was imposed at the tank walls and heater surfaces. All solid surfaces were treated as adiabatic and heat and mass transfer between liquid and vapor phases were neglected.

There was some cell clustering across the diameter of the jet (approximately 6 cells across the diameter). There was a trade in the simulation between trying to capture the spreading of the jet and providing a nearly uniform grid at the ullage interface which provides the best accuracy from the surface tracking algorithms. Turbulence was modeled with a two equation k- ϵ approach. Surface tension was modeled implicitly using a 5° contact angle. Surface tracking used an un-split Lagrangian model. The momentum advection model was 2nd order. The LAD was modeled as a distributed sink with a total flow rate equal to flow issuing from the jet. The gap between the tank wall and LAD was not modeled. Although the code has the capability to model the heat addition from the internal tank heaters as well as the accelerations caused by pump vibrations and reaction control thruster firings, no attempt was made to model those phenomena in these preliminary simulations.

The video at the beginning of the jet mixing portion of each Test Run simulated was used to approximately define the ullage bubble location. The ullage bubble size was determined by the experimental fill fraction. The ullage shape is initialized as a spherical bubble, but 20 seconds without jet mixing are simulated to allow the ullage shape to reach an approximate equilibrium shape before the jet is activated in the CFD simulation. The acceleration during the TPCE experiments was predominantly along the long axis of the tank. For the CFD simulations, the acceleration magnitude was approximated as a constant value of 1.0×10^{-6} g and a constant direction along the long tank axis.

IV. Simulation Results

Figures 4-6 show the ullage dynamics during the jet mixing process for Test Runs 11, 15 and 13, respectively. The simulation results used adiabatic surfaces (including the two heater plates) and did not include the self-pressurization period of each test run. The upper right hand corner of each figure shows the surface contour of the fluid fraction which indicates the location of the liquid/ullage interface. The upper left hand corner shows a still image taken from the video of a TPCE run. The bottom two images in Figures 4-6 are cross sectional cuts through the tank showing contours of fluid fraction.

Figure 4 shows results for Test Run 11 with a jet Weber number of .71 and a flow rate reported as 0.59 L/min. At the beginning of this test, the ullage is assumed to be attached to both the top of the tank and the side heater. The test was classified as non-penetrating since the jet never penetrates completely through the ullage but creates an indentation at the liquid ullage interface. In the simulation (Figure 4.), the jet never penetrates through the ullage for the approximately 240 s of simulation time corresponding to the duration of the test. In Figure 4., the simulation also captures the attachment of the ullage to the side heater although residual thermal effects from heating were not modeled. An indentation is created in the ullage where the flow from the jet meets the ullage and is contained at the interface. In the simulation, this indentation remains very stable. However, in the experiment, the indentation exhibits substantial motion. This motion is illustrated by comparing the ullage interfaces at times $t = 55$ s and $t = 101$ s in Figure 4. It is unclear if this motion is due to forces external to the experiment (i.e. pump vibration, thruster firings, or convective currents from the heaters) or if the simulation lacked the fidelity to capture this motion due to excessive damping at the interface or the inability to capture unsteadiness in the jet.

Figure 5 shows results for Test Run 15 with a jet Weber number of 4.74 and a reported flow rate of 1.53 L/min and was classified as an asymmetric case. In an asymmetric experimental case, the ullage is ultimately pushed to one side of the tank after being penetrated by the jet. A comparison of the jet penetration seen in the experiment and that in the simulation is shown in Figure 5. Unlike the jet flow of Test Run 11, the jet flow is of sufficient strength to fully penetrate the ullage as seen in both the experiment and simulation ($t = 25$ s). The simulation captures ($t = 71$ s) the large funneled shaped penetration seen in the experiment. At 71 seconds, it is clear that the simulation captures the penetrating jet flow that flows through and behind the ullage and keeps it from attaching to the tank dome. In the simulation, the ullage first moves toward the top tank heater (unlike the experiment) before it finally settles down on the same side (bottom $t = 203$ s) as seen in the experiment.

Figure 6 shows results for Test Run 13 is the highest jet flow rate case simulated. The jet flow rate was reported as 2.78 L/min which would correspond to a jet Weber number of 15.55. Run 13 is classified as a penetration case. In a penetration case, the jet quickly goes through the ullage and is diverted back around the ullage by the tank dome. As the jet penetrates the ullage and is diverted by the dome, the ullage forms a very irregular shape. Figure 6. shows a comparison of the simulation of the jet penetration with the experiment. It is seen that at time $t = 23$ s, in the top left hand image, the jet penetrates the ullage. The face of the ullage towards the jet is flattened. The simulation produces a more pinched ullage shape than the spherical shape maintained by the ullage at

this time. At $t = 25$ s, both the experiment and the simulation exhibit a pinched, key shaped ullage. At $t = 55$ s, some gas is detached from the main ullage bubble in both the experiment and simulation. As the simulation progresses ($t = 116$ s), the simulation captures the rotation of the ullage to the side (bottom) of the tank as seen in the experiment.

A CFD simulation was also performed of Test Run 4 in hopes of getting a more quantitative comparison of the simulation results with the experiment. The jet flow rate for Run 4 is 1.53 L/min for a jet Weber number of 4.73. It is classified as an asymmetric case. In Test Run 4, the ullage is situated in the center of the tank attached to the side heater. As the jet penetrates the ullage and emerges on the other side, a liquid protuberance is formed (Figure 7) that eventually collides with the tank dome. The simulation qualitatively captures the development of the ullage protuberance created by the jet, the continuing attachment to the side heater, and the wedge shape of the ullage. Images of the experiment were digitized, and the protuberance's distance from the tank dome (Figure 8) was quantified for comparison with simulation results. However, it was evident that the progression of the protuberance slows ($t = 1.5$ s to 2.5 s in Figure 8) and then accelerates again. This behavior was not captured in the simulation. It is hypothesized that this may be an optical artifact of the experimental setup (the image of the Cartesian grid placed behind the tank being refracted).

V. Summary

The simulations qualitatively reproduce the ullage dynamics for various jet mixing flow rates and ullage starting positions as seen in the TPCE experiments. The current simulations do not include the thermal effects of the heaters. Quantitative comparisons of the simulations with the experiments may need to include simulation of optical effects.

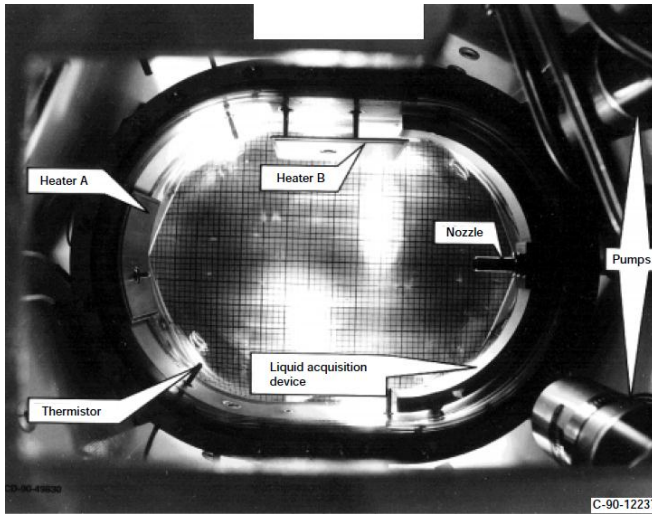


Figure 1. – TPCE experimental hardware.

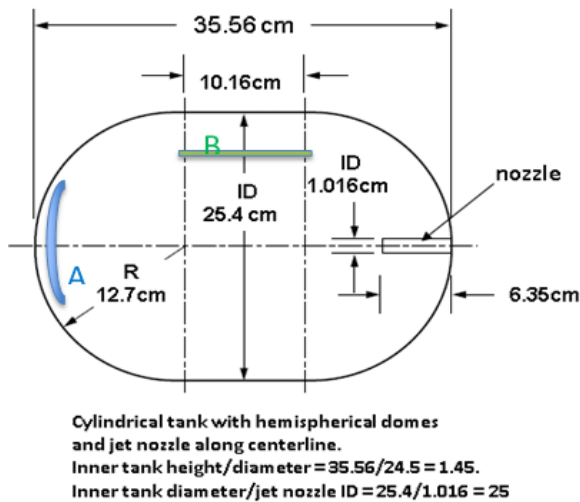
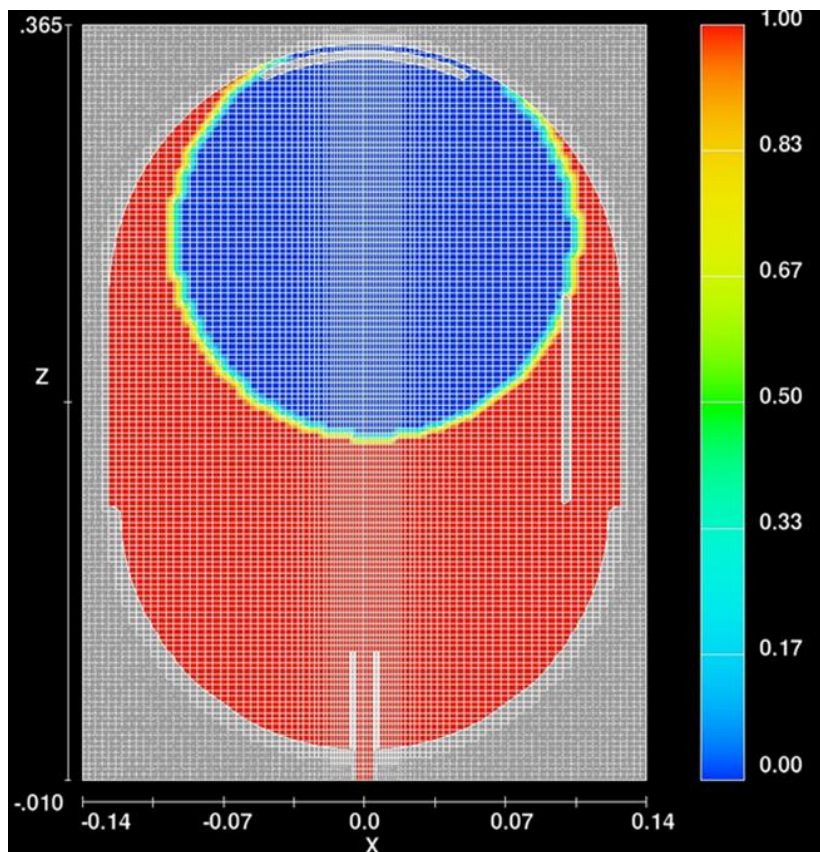
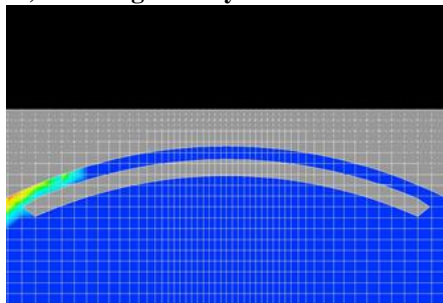


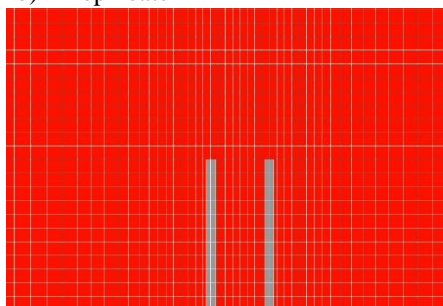
Figure 2. – TPCE tank geometry and dimensions.



a) Tank geometry

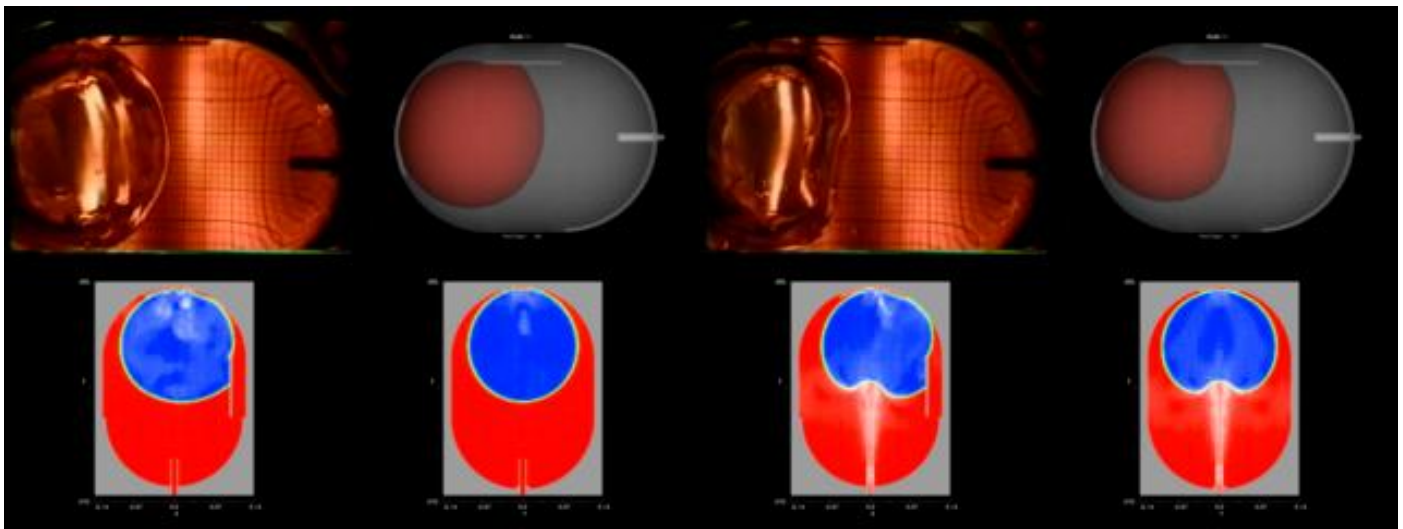


b) Top heater



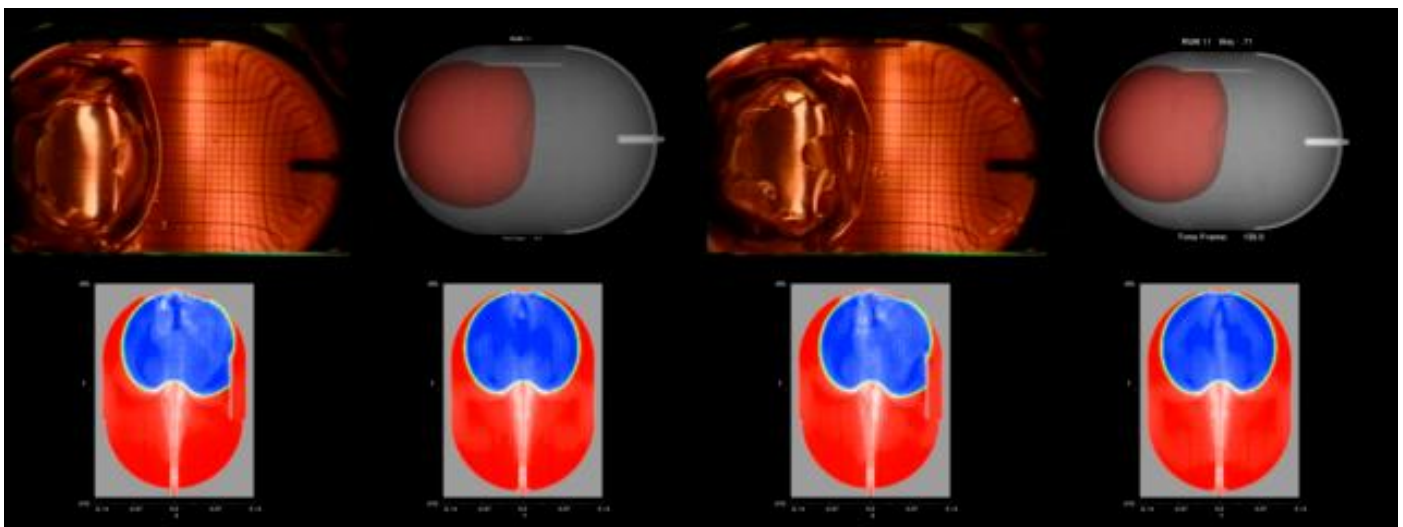
c) Jet exit

Figure 3. – Fluid fraction and clustered Cartesian grid [742,000 active cells (dimensions in meters)].



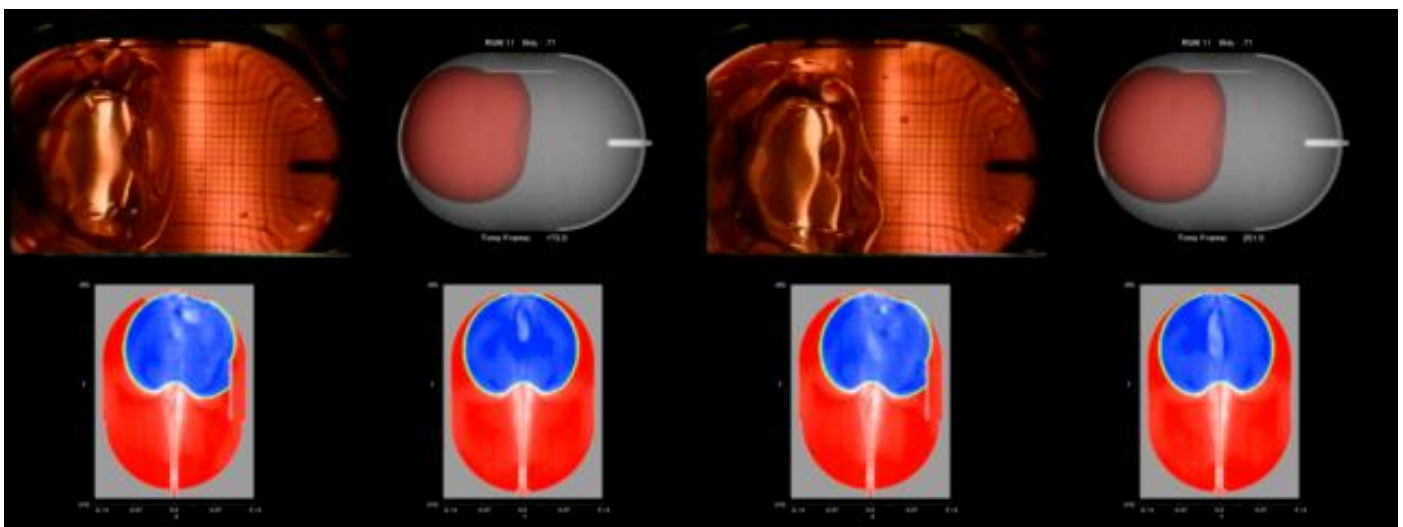
$t=20s$

$t=55s$



$t=90s$

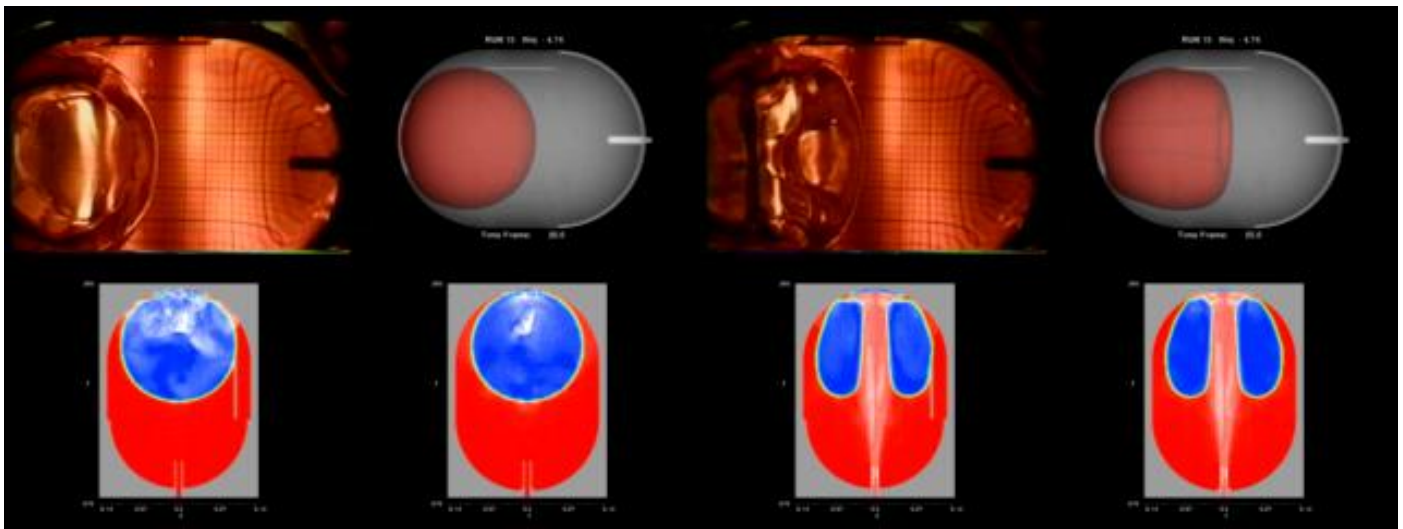
$t=101s$



$t=180s$

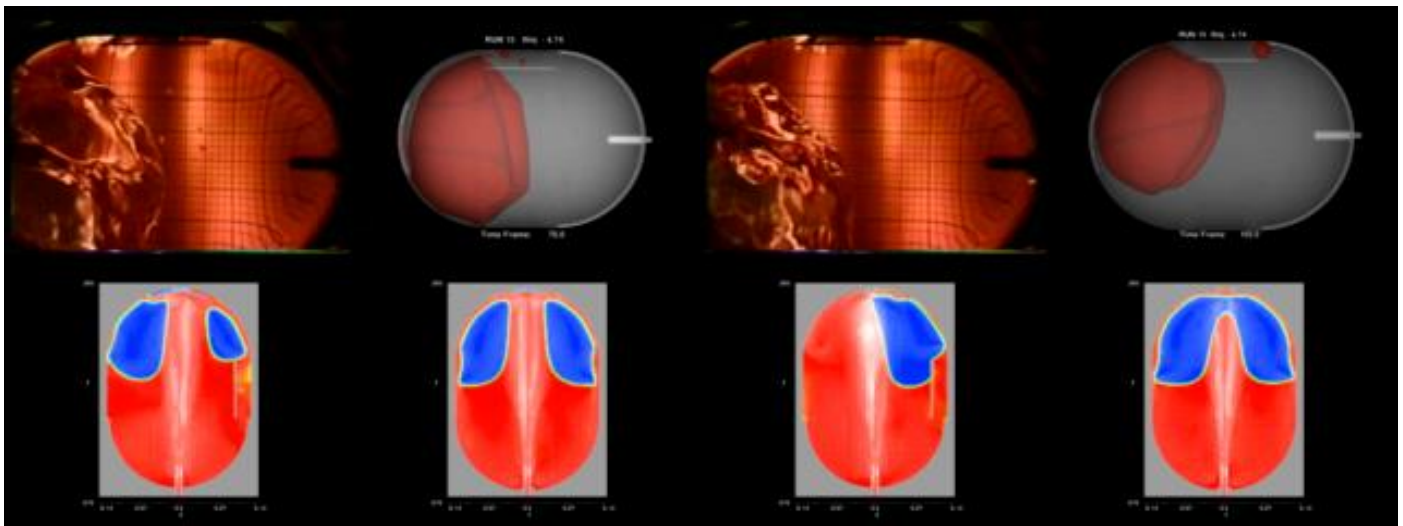
$t=261s$

Figure 4. - Run 11 experimental ullage images and simulation contours.



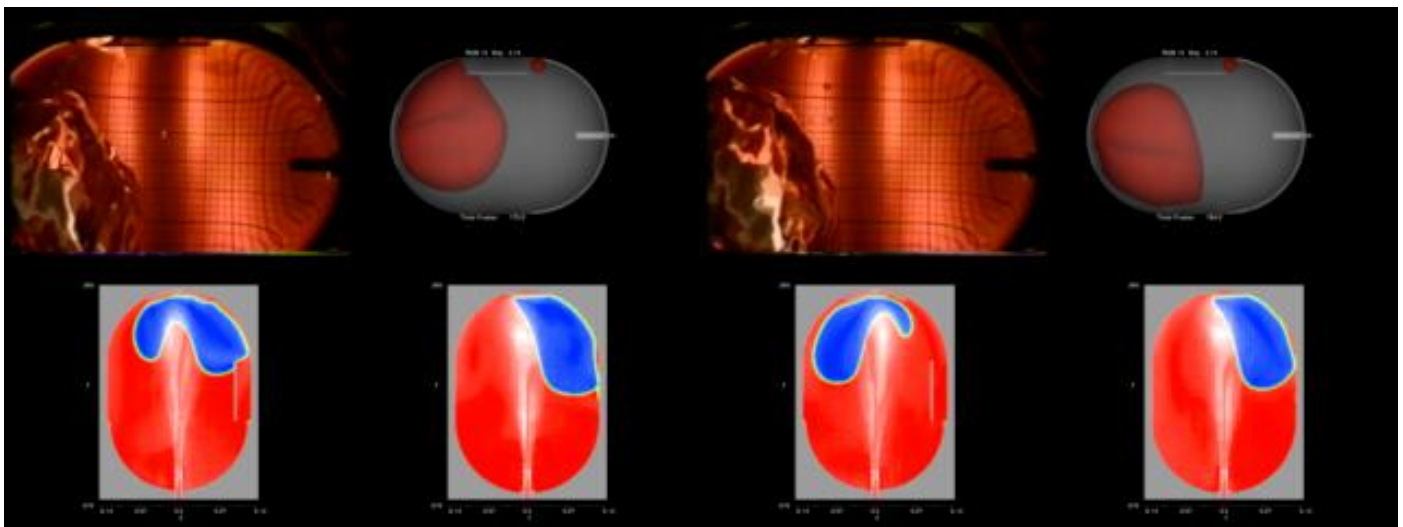
$t=20s$

$t=25s$



$t=71s$

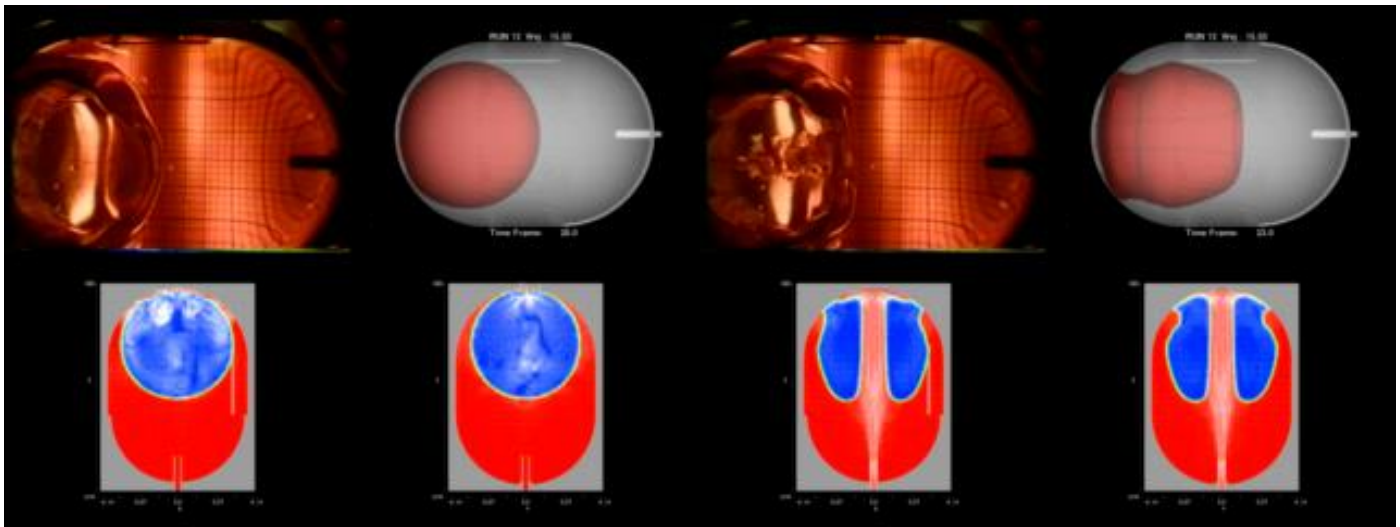
$t=104s$



$t=173s$

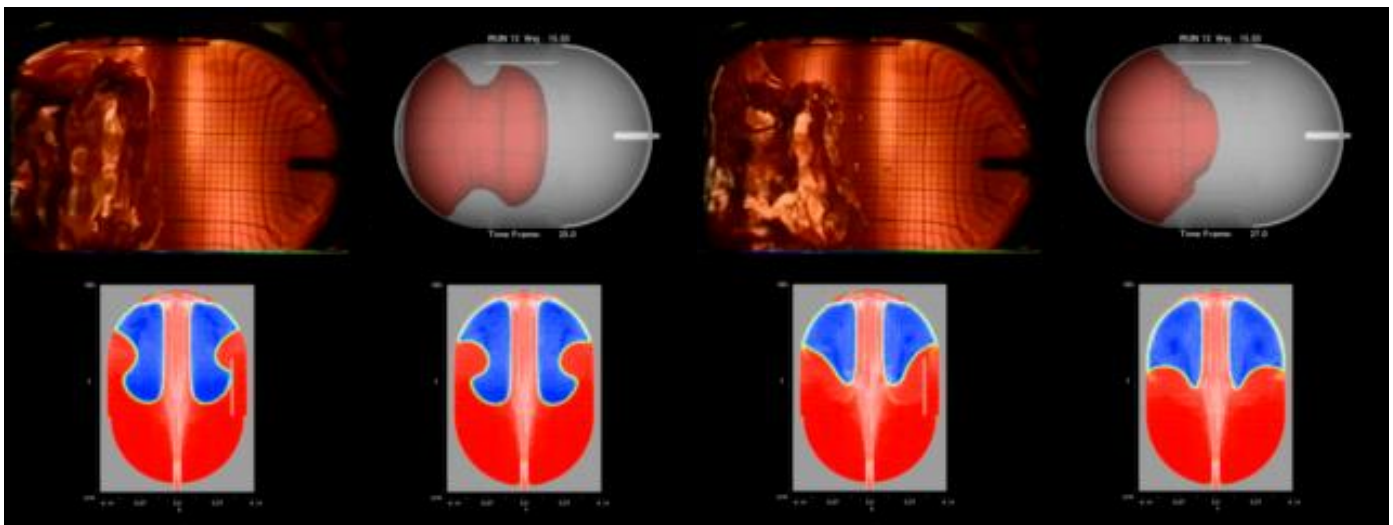
$t=203s$

Figure 5. - Run 15 experimental ullage images and simulation contours.



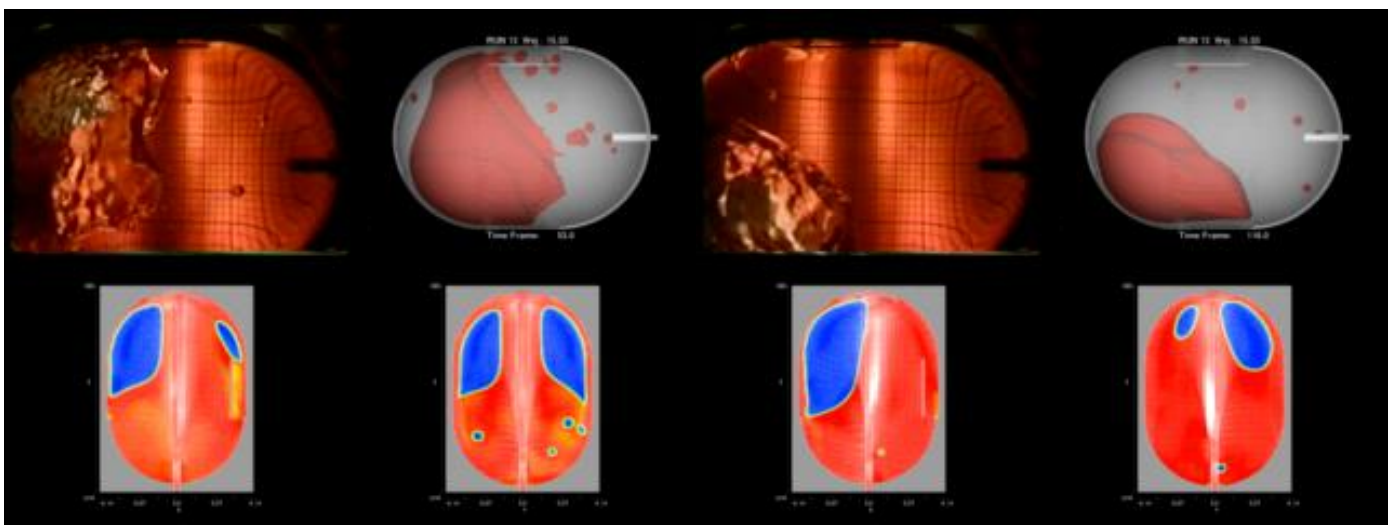
$t = 20\text{s}$

$t = 23\text{s}$



$t = 25\text{s}$

$t = 27\text{s}$



$t = 53\text{s}$

$t = 116\text{s}$

Figure 6. - Run 13 experimental ullage images and simulation contours.

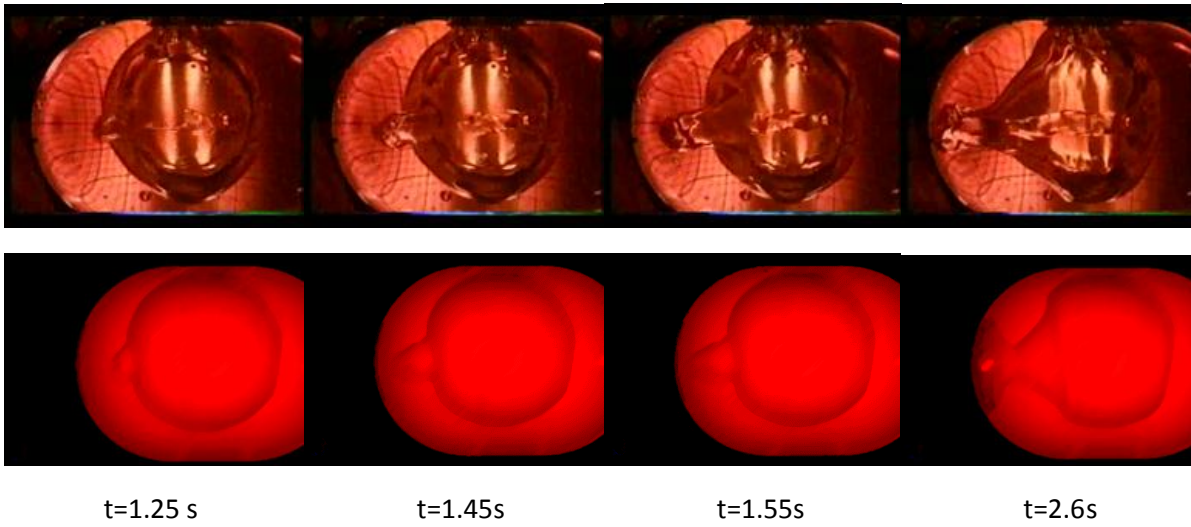


Figure 7. – Comparison of simulation and experiment for RUN 4 ullage anchored at side heater.

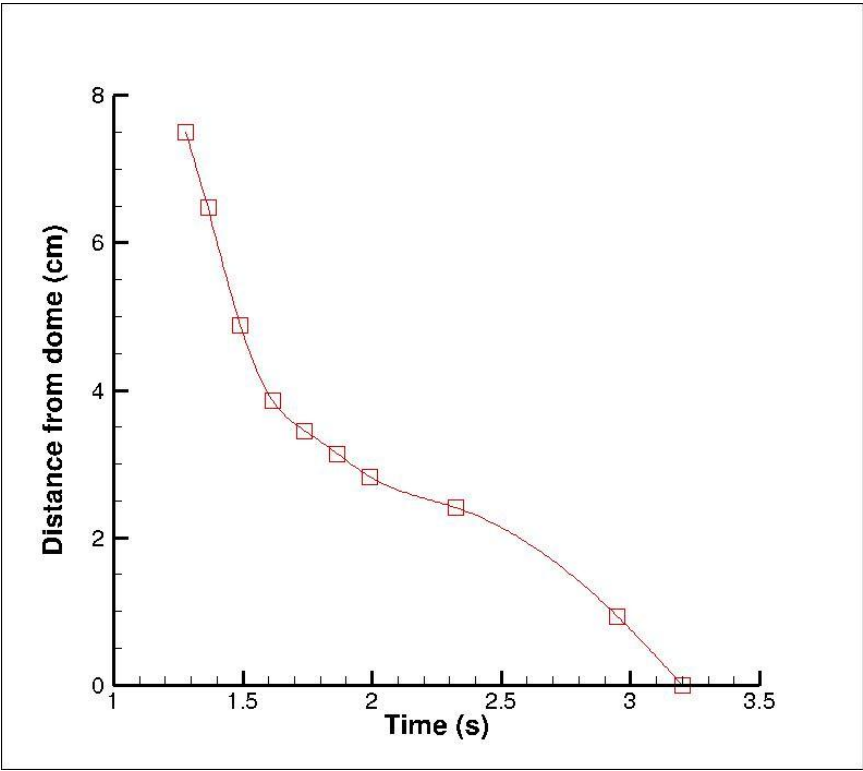


Figure 8. – Jet protuberance from ullage for Test 4 (from digitized images)

References

- [1] “Tank Pressure Control in Low Gravity by Jet Mixing”, Benz, M., NASA CR 191012, March 1993.
- [2] “Modeling of Jet-Induced Geyser Formation in a Reduced Gravity Environment “ , Wendl , M. C., Hochstein, J. I. and Sasmal, G. P., AIAA-1991-803, 1991.
- [3] “Modeling of Space Vehicle Propellant Mixing”, Aydelott, John C., NASA TP-2107, January 1983.